Defence Oceanology International '91 Exhibition & Conference **6-8 March 1991, Brighton (U.K.)**

THE "CRYO-THERMAL" CLOSED CYCLE DIESEL ENGINE

DETAILED ANALYSIS OF STATIONARY WORKING CONDITIONS

Attilio Brighenti[1]
Giuseppe Cantore[2]
Paolo Osti[3]

ABSTRACT

The "*cryothermal engine* " is a closed cycle Diesel system in which exhaust gases are cooled and part of them compressed so that CO_2 is condensed, separated and stored at low temperature, thanks to heat exchange with stored liquid oxygen. This generates a cooling effect while is evaporated and superheated to feed the inlet mixture of the engine. The system, patented in a number of countries, was presented in a previous paper where the main differences and advantages were shown with respect to other energy systems for Autonomous Underwater Vehicles (AUV). Basic thermodynamics and performances of the plant were presented and discussed, highlighting the high degree of system's non linearity.

This paper is the result of a further design and analysis work performed by means of a specially developed computer model which solves in the time domain the whole set of differential equations governing the process and its control; this model allows extensive analysis of both *stationary and dynamic* conditions of the system under various environmental and time varying load conditions and control set points.

The object of this paper is an overall description of the model focusing on the discussion of the *stationary* conditions of a system designed to deliver 12 kW peak power and 600 kWh energy; these performances are typical of a long range AUV. The simulated conditions span the whole Torque-Speed diagram of the engine.

Diagrams of temperature, pressure, gas mixture composition, flow rate, in the most significant plant sections, and of the compressor power and its ratio to the engine power are presented. The results obtained confirm the expected performance and the high flexibility of the *cryothermal engine* and of its control system. In particular the efficiency of the separation process for the combustion products is as high as predicted by previous basic analyses over a large field of the engine torque-rpm diagram. The power lost due to excess gas compression is less than 10 % of the engine power for high torques, falling below 8 % at maximum torque conditions.

---

1 MSc, Mech. Eng., Research and Development, Manager, Systems,Tecnomare SpA, Venice
2 Msc, Mech. Eng., Associate Professor at the Institute of Machines, University of Bologna
3 MSc, Mech. Eng., Research Fellow at the Institute of Machines, University of Bologna

1 INTRODUCTION

Closed cycle Diesel systems have been the object of various research and development activities and are proposed mainly for the propulsion of underwater vehicles, most often of the manned type.

Various technical solutions have been identified in the two main problem areas of this technology [2, 3, 5, 6, 7, 8, 9, 10, 13, 14, 15, 16]:

- The engine, working with an artificial mixture;
- The treatment of the exhaust gases produced by the combustion.

While studying a possible application of this technology to deep water unmanned vehicles, a new closed cycle solution based on the liquefaction of CO_2 at low temperature was identified. This solution is based on the use of liquid oxygen (LOX) as the oxidant stored on board.

Previous papers on this subject by the principal author and others [2, 3, 4] described the system, the result of preliminary thermodynamic and control system analyses and its advantages with respect to other known systems. It was shown that the cryogenic liquefaction allows a true depth independence, lower weight and volume and a sensibly lower loss of engine power to treat the exhaust gases produced. The specific energy achievable with this system is 350 Wh/kg with the equipment designed for the atmospheric environment. If the systems induce pressure resistant vessels for the engine, the reactants and the combustion products suitable for 6000 m water depth, the specific energy is reduced to ca. 100 Wh/Kg, still much higher than values obtainable with any rechargeable battery and only inferior to some primary batteries and Hydrox fuel cells, provided, for the latter, that oxygen and hydrogen are stored as liquids.

Also the high non linearity of the whole system was highlighted. This implies the need for a numerical model to study the system's performance under both stationary and transient load conditions.

The work undertaken by the authors resulted in the development and validation of the model, by comparison with previous results and theoretical analyses. Also extensive stationary and dynamic simulations of a typical system for an Autonomous Underwater Vehicle were run.

This paper describes the basic aspects of the model and the results obtained in the stationary conditions analyses.

2 SYSTEM DESCRIPTION

Fig. 1 shows the process diagram of the "Cryo-thermal"[1] closed cycle Diesel engine. On the left side is shown a modified engine working on a binary CO_2/O_2 mixture[2], discharging at low pressure (from 1 to 2 bar).

The right side of the system is instead a gas management system, composed of the following main components:

- two insulated cryogenic storage vessels, the oxygen one being installed above the carbon dioxide one; inside this is installed the 2nd stage CO_2 condenser, cooled by oxygen;
- one liquefaction loop (warm side) with condensated water separator, compressor, post compression water-cooler, filters and dehydrators, counter-flow cryogenic cooler and 1st stage condenser;
- one oxidant mixing manifold which collects both the pure oxygen and the residual, oxygen rich, uncondensated gas coming from the CO_2 vessel.

The latter function allows a total recovery of the oxygen unburnt by the engine, thus maximum energy obtained from the oxygen stored.

The engine exhausts are cooled from about 450°C down to ca 20 °C by secondary fresh water, sprayed in counter-flow to allow separation of solid or liquid particles trapped in the gas stream. Combustion water is condensed and separated; the gas, which contains residual oxygen, is sent to the mixer where fresh oxygen is added by a regulator. A fraction of the recirculated and dehumidified gas is deviated by the two stage electric compressor, activated by the pressure control loop in the water separator. Down-stream to it, the dehydrating filter and the post-compression water cooler allow the compressed gas to enter the cryogenic section free of water and at the minimum temperature achievable with sea water.

The CO_2/O_2 mixture enters the surface heat exchanger in counter-flow with oxygen vapour, which is superheated from ca -180 up to 0°C or higher. On the other side CO_2 starts condensating and completes the process (at ca -45 °C) within the low temperature condenser and storage tank, coming into contact with the second heat exchanger in which liquid oxygen evaporates. The flow in this evaporation loop is returned to the oxygen tank by natural circulation, thus cryogenic pumps are not needed in the system. This flow is controlled by the on/off solenoid valve actuated to maintain constant gas pressure in the oxygen tank.

The residual gas uncondensated in the CO_2 tank, which is an oxygen rich binary

---

1 System patented

2 The gas management system can work however with other engines, such as Diesel on a ternary mixture (i.e. with Argon or Nitrogen and CO_2 as inerts) or Stirling, with proper modifications as mentioned in ref. [3].

mixture, is vented to the oxygen mixing manifold. Venting is controlled by the regulation loop fed-back by the pressure and the temperature in the CO_2 tank.
The plant's control system includes five loops of the following types:

Parameter	Control type	Actuator
- oxygen concentration in the mixing manifold	PID	Oxygen valve
- c.c. engine loop pressure	P	Compressor
- CO_2 tank pressure	P	Venting valve
- Oxygen tank pressure	ON/OFF	LOX valve
- engine speed	PI	Standard rpm regulator

3 MODEL DESCRIPTION

Need for a model

In a previous work [2] the system was defined by 27 equations of as many variables. Linearization at given load conditions resulted in 275 linearization constants whose values depend on engine working conditions. That study allowed the fixing of tentative control loop gains and the analysis of the system's non linearity. Constants sensitivity analyses and classification showed those subjected to largest changes with the load torque and engine speed set point. Five to fourteen "constants" showed a relative variation 30 % higher than input relative variation. For two of them the figure was about 70 %.
Therefore one critical point before entering an experimental phase is first to verify whether the above mentioned simple, single loop, controllers would perform properly even under these system non linearities. In case a multivariable control system is finally used, a test bench model is necessary prior to application to the real plant. This suggested the development of a time domain complete model, based on the whole system of non linear differential equations.
Another important aspect, which is the focus of this paper, was to verify the performances of the complete system over the full spectrum of engine working conditions, both stationary and dynamic, to confirm the expected efficiency of the gas treatment and storage unit. Indeed in the previous work this unit was studied independently of the engine, with interface conditions set as input to a simple thermodynamic model of the liquefaction unit. Now the model incorporates also the engine block and allows the accounting for changes in the exhaust gas composition and temperature at various loads and system set points.

The dynamic model

The system is described in the present model by 141 non linear equations defining 12 state variables and 129 auxiliary variables (see a partial list and definitions in the appendix). The state variables correspond to as many differential equations (among the above 141) and to the system's physical elements where energy accumulation occurs under dynamic conditions and to the derived control variables of the regulators. The former are listed in the following table:

Element	Type of energy	Physical variable involved
Engine moment of inertia	kinetic	rotational velocity
Oxygen mixing manifold	enthalpy	pressure temperature Oxygen concentration[1]
Exhaust water condenser	enthalpy	pressure[2]
Compressor mom. of inertia	kinetic	rotational velocity
CO_2 condenser & stor. vessel	enthalpy	total pressure temperature[3]
LOX storage vessel	enthalpy	pressure[4]

Independent energy accumulation in pipes and heat exchangers is disregarded in this model. Their volume however is added to that of the adjacent elements, as a contribution to internal energy; instead thermal energy accumulation in the heat

1 This element is bi-component with a gaseous phase mixture. The three variables can therefore vary independently of each other in the time, following the three flow inputs and the single flow output.

2 This element is actually tri-component: O_2 , CO_2 , H_2O. This would define in principle 4 state variables: H_2O vapour and O_2 concentrations, temperature and pressure of the gas mixture. The model however considers only the pressure as a state variable, which must be controlled. The other 3 variables are included in the equations as auxiliary variables, in phase with the corresponding ones at the element inlet. Dynamic simulations showed very small and slow variations of these 3 quantities, thus the validity of the simplification.

3 The condition of CO_2 liquid-vapour equilibrium is assumed in the present model, thus the third state variable theoretically associated to this bi-component element is eliminated by the corresponding relationship.

4 Also in this case the liquid-vapour equilibrium is assumed and the state variable for this mono-component element is one (the pressure).

exchangers (e.g. in the materials) and the relevant transients are disregarded. This is equivalent to assuming that the flows through the heat exchangers are at each time in equilibrium and the temperatures are those obtained under stationary conditions.

Dynamic simulations have shown that even under sharp torque or rpm set point variations the temperatures vary very slowly, so that the assumption of *quasi-static* behaviour of these elements does not invalidate the model.

In conclusion the number of physical state variables is 9.

In addition to these other 3 state variables are associated to the control loops equations (2 for the PID, 1 for the PI controller), thus the total number of state variables and the minimum of differential equations needed to describe the system sum up to 12. The 129 auxiliary variables mentioned above are instead associated to as many non differential, non linear equations, which are left explicit in the model. These 129 variables are "in phase" with the state variables included in the same auxiliary equations.

The solution of this system of equations is performed by a specially developed computer program using either a fourth order Runge-Kutta or Milne predictor-corrector methods, with variable time steps set as an input vector.

The starting state for system's dynamic simulation is calculated first with iterative routines dedicated to the solution of the stationary conditions.

The program runs on PC and its general block diagram is shown in Fig. 2.

4 ANALYSIS OF THE STATIONARY CONDITIONS

One system's design case and related simulations were finalized to an Autonomous Underwater Vehicle (AUV) for long range surveys close to the ocean floor (Fig. 3). The energy system requirements of said typical vehicle are reported in Table 1.

The engine characteristic curves (torque, power, specific fuel consumption vs rpm) are those of a commercial two-cylinder Diesel engine, modified to work with a CO_2/O_2 gas mixture (77/23 % in mass)[1]. The curves, shown in Figs 4 and 5 are derived from the experimental curves of the engine working on air[2].

Other most significant input data are the set points of the regulators and the environmental conditions, reported in Table 2.

The first step in the stationary conditions analysis was to verify the previous results [2] relative to the dependence of the liquefaction system performance on the *mass flow rate* (f) parameter. This is the non-dimensional ratio between the actual gas

---

[1] Refs. 3, 9 and 10 give an overview of the main aspects of Diesel engines operating with artificial mixtures.

[2] The corresponding function equations are program subroutines that can be easily changed in the simulation program, depending on the engine adopted.

flow rate delivered by the compressor and its theoretical minimum value. This minimum would correspond to a net CO_2 flow rate through the compressor equal to that produced by engine's combustion at given torque and rpm. Under these limit conditions the gas vented from the CO_2 vessel would be pure oxygen. In real cases f is always greater than unity, as non condensed CO_2 is discharged from that vent, thus the compressor is required to deliver a corresponding surplus flow capacity.
The above concept can be expressed in formulas by the following equations:

(1) $$f = \frac{m_{de}}{m_{de_{min}}} > 1$$

where m_{de} is the flow rate through the compressor, whose minimum is:

(2) $$m_{de_{min}} = \frac{Bf\, m_{ox}}{1 - g_{de_{ox}}}$$

where:

Bf is the mass of CO_2 produced by the combustion of the fuel with 1 kg of oxygen (Bf = 0.892 for Diesel fuels).

m_{ox} is the oxygen flow rate for the assigned engine output and speed

$g_{de_{ox}}$ is the oxygen mass concentration in the mixture delivered by the compressor.

The oxygen concentration at the CO_2 vessel vent ($g_{i_{ox}}$) is defined univocally as function of f and $g_{de_{ox}}$:

(3) $$g_{i_{ox}} = \frac{f\, g_{de_{ox}}}{f - 1 + g_{de_{ox}}}$$

Under stationary conditions the quantities m_{ox} and $g_{de_{ox}}$ are given by the engine equations. The parameter f, or the excess compressor delivery, can be chosen arbitrarily for same engine outputs, but it is an optimization factor of process efficiency, as was found in the previous work [2]. The simulations performed in this work confirmed both qualitatively and quantitatively those results.
Figs 6 and 7 show the dependence of pressure and temperature in the CO_2 liquefaction system, while Fig. 8 shows the compressor power consumption as a percentage of engine power[1], for two extreme shaft torque and speed set points, corresponding to the minimum and maximum power. The minimum of condensation start temperature and corresponding total pressure, for f = 1.5 and 1.3 respectively

[1] CLF is for Compression Power Loss

can be seen .

Accordingly the compressor power features a minimum for $f = 1.1 \div 1.15$.

After this analysis an extensive sensitivity analysis of the process parameters has been performed for same environmental conditions, spanning the whole engine torque-rpm working area; Fig. 9 shows the points of the stationary simulations which are grouped in curves of constant rpm. The mass flow rate was kept constant in all these simulations. Diagrams of some most interesting parameters are reported in Figs. 10 through 19.

In Figs. 10 and 11 are shown the dependence with evident minima of the vapour pressure (p_{pcd}) and temperature (T_{sc}) in the CO_2 pressure vessel vs the engine torque. This can be explained by the existence of two counteracting factors.

The first *factor* is that oxygen consumption is proportional to the torque for any given speed (Fig. 12), while heat losses through the vessels thermal insulation are almost constant[1]. This implies that at low torque a higher fraction of the cooling power made available for the liquefaction of the CO_2 by the oxygen flow is lost by this heat leakage. As a consequence the CO_2 end condensation temperature and vapour pressure must be higher to allow a reduction of the condensation enthalpy and satisfy the balance; therefore they both increase at low torques, more sharply at lower engine speeds and corresponding lower oxygen demand.

The *second factor*, responsible for the opposite trend, is the reduction in the oxygen superheater efficiency due to the increased flow on both sides, the oxygen's and the compressed exhausts'. This is evident from Fig.13 showing the decrease of oxygen exit temperature (T_3) at high torques. Consequently the overall cooling effect by the oxygen reduces at increasing torque, thus the thermal balance can be satisfied only at higher CO_2 condensation temperature and pressure, again for the lower enthalpy of condensation implied.

The two factors described above are acting together, the former being predominant at low torques and low rpm, the latter at high torques and rpm. The overall effect is that temperature and CO_2 partial pressure in the condensator and storage vessel show a minimum at torque values which depend on the engine speed (Figs. 10 and 11), the higher the rpm, the lower the torque of minimum.

The total pressure in the CO_2 vessel (p_{sc}), thus compressor's outlet, is shown in Fig. 14, which is of course correlated to the oxygen concentration in the exhaust gas (Fig. 15) and in the uncondensated gas vented (Fig. 16).

Another important result is the compressor flow capacity and power shown in Figs. 17 to 19; from the last one in particular is seen that this power loss due to the

---

[1] The heat flow towards the cryogenic LOX vessel is about 3.2 to 3.7 times that exhibited by the CO_2 vessel. The latter changes with CO_2 temperature and engine load, while the former is constant as the temperature and pressure are kept constant by the control system.

liquefaction process is below 10 % of engine's over a wide set of load conditions, and most importantly decreases with torque. The highest values (max 13 %) can be tolerated as they are associated to low absolute power losses (less than 0.4 kW) and do not reduce dramatically the net energy capacity of the system. It must be remembered however that these simulations were perfomed with a manifold pressure set at about 1 bar and with the flow rate parameter (f) set at 1.3, thus above the optimum value for low power losses (see Fig. 8). Should the latter be set at ca 1.1 ÷ 1.15 and the former at 2 bar, providing the engine is suitable to supercharged pressure conditions, the Compressor Loss Factor (CLF) would be even lower, typically 30 % less.

5 CONCLUSIONS

The study and the work performed produced an essential tool for the comprehension of the behaviour, the design and tests planning of the "Cryo-thermal" closed cycle Diesel system, using a low temperature liquefaction process to separate the combustion products from the gas mixture and store them in limited volumes. One important result obtained from the detailed model developed is the confirmation that the liquefaction process power demand is a very low fraction of engine power, namely below 10 % at medium to high torques, most importantly with the highest percentages associated with the lowest absolute values. This holds true over the full spectrum of working conditions, which is one of the main advantages of this system [2]. Also the temperatures and pressures at various points of the process are in line with the expected performances: CO_2 condensates at temperatures around -45 °C and the total pressure of the gas mixture is between 13 and 32 bar, depending on engine working conditions.

The above leads to the conclusion that the system is feasible, and that the advantages previously cited over other closed cycle Diesel technologies are confirmed.

Future work in this area will deal with a more detailed and correct simulation of the thermodynamic cycle of the engine to update the torque-speed relationship used in this model. Also an experimental phase will be undertaken to fully validate both the closed cycle and the engine cycle models.

REFERENCES

[1] Brighenti A.: "System for the Treatment and Cryogenic Storage of Combustion Products of Thermal Engines", 1987 Italian Patent n. 22885 (extensions pending);

[2] Brighenti A., Minelli G., Dalla Rosa A.: "The Cryo-thermal Engine underwater power system: performances, dynamics and control", Oceans '89 Conf., Seattle (WA), Sep. 1989;

[3] Brighenti A., Ciliberto G.: "I motori alternativi elettrogeni a ciclo chiuso nella navigazione subacquea dei mezzi sottomarini", Seminar of the Associazione Termotecnica Italiana (Sez. Venezia Giulia), Trieste, 20 Feb. 1989 (paper being published).

[4] Brighenti A.: "Parametric analysis of the configuration of autonomous underwater vehicles", IEEE Journal of Oceanic Engineering, Vol. 15, n. 3 July 1990, pp. 179-188.

[5] Brunner G.: "Internal combustion engine with exhaust gas recycling system and method for operating such engine", 1974 U.S. Patent n. 1,513,958.
[6] Fowler A., Boyes A.:"The Argo-Diesel Enhanced Underwater Power Source", Underwater Technology Conference, Bergen (N), 1987;
[7] Haas J.:"Air Independent Power Sources of High Energy Storage Density. The Bruker-Man Argon Diesel and the Bruker CO_2-Diesel", 3rd Hydrocarbon Symposium, Luxembourgh, Mar 1988;
[8] Hoffman L.C. & others: "Psychrocycle", Marine Technology Society Journal, v.4 n.6 Nov.-Dec. 1970;
[9] Nagai M., Asada T.: "Investigations on Recycle and Closed Cycle Diesel Engines", 12th International Congress on Combustion Engine, Tokyo, May 1977;
[10] Nagai M., Asada T.: "Investigations on Recycle and Closed Cycle Diesel Engines", SAE paper n. 800964;
[11] Obara T. & others: "A New Closed Circuit Diesel Engine for Underwater Power", ROV '89 Conference, San Diego (Cal), Mar '89;
[12] Prins C.A., Ham A.A. "In search of air independence", Maritime Defence, Mar. '88
[13] Puttick J.R.:"Recycle Diesel Underwater Powerplants", Paper 710827 SAE National Combined Fuels and Lubricants, Powerplants and Truck Meeting, St Louis (Mo) Oct. 1971;
[14] Santi G.:"PHX Submersible", Subtech 1983 International Conference, Society of Underwater Technology, London, 1983;
[15] Thompson R.V. & others "The Development of a Microprocessor Controlled Depth Independent Power Generation System", Pergamon Press Oxford & N.Y. 1980;
[16] Thompson R.V., Fowler A. "Development of a Depth Independent Closed Cycle Diesel Engine", Offshore Technology Conference Paper n. 4031, Houston, May 1981.

APPENDIX - MAIN SYSTEM EQUATIONS AND VARIABLE DEFINITIONS

In the following the 9 differential equations defining the system behaviour are shown. They refer to the 7 physical elements of the system where energy accumulation occurs under dynamic conditions. These are complemented by the 3 differential equations of the PID and PI regulators and the 129 auxiliary equations, which allow the solution of the system (i.e. the equations of the thermodynamic properties of gas components as function of the state variables, the state equations in the various systems parts, thermodynamic work relationship, etc.).
Bold characters indicate the state variables. Most of them are not explicited in the equations as they are linked to the derivated function by several auxiliary rcalationships.

Equations — Time dependant variables

Block 1 - Engine

1.1: shaft balance

$$\frac{d\boldsymbol{n}}{d\tau} = \frac{60}{2\pi J}\left[C_m(\boldsymbol{n}, g_r) - C_r\right] \qquad \boldsymbol{n},\ C_m,\ g_r$$

Other 12 (auxiliary) equations in this block define the relationship $C_m = C_m(\boldsymbol{n}, g_r)$ and those between the above variables and inlet, outlet gas and fuel mass flow rates on one side and density, exhaust gas temperature, specific heat at constant volume and gas constant, O_2 and H_2O concentration on the other.

Equations | Time dependant variables

Block 2 - Oxygen mixing manifold and residual oxygen collecting manifold (OMM and ROCM in Fig. 1)

2.1: mass balance

$$\frac{dM_b\,(p_b,\,T_b,\,g_{s_{ox}})}{d\tau} = \dot{m}_{ox} + \dot{m}_i + \dot{m}_r - \dot{m}_s$$

$M_b, \dot{m}_{ox}, \dot{m}_i, \dot{m}_r, \dot{m}_s$

2.2: enthalpy balance

$$\frac{dU_b\,(p_b,\,T_b,\,g_{s_{ox}})}{d\tau} = \dot{m}_{ox}\,h_3 + \dot{m}_i\,h_4 + \dot{m}_r\,h_r - \dot{m}_s\,h_s$$

$U_b, h_3, h_4, h_r, h_s, \dot{m}_{ox}, \dot{m}_i, \dot{m}_r, \dot{m}_s$

2.3: oxygen mass balance

$$\frac{dM_{ox}\,(p_b,\,T_b,\,g_{s_{ox}})}{d\tau} = \dot{m}_{ox} + g_{i_{ox}}\,\dot{m}_i + g_{de_{ox}}\,\dot{m}_r - g_{s_{ox}}\,\dot{m}_s$$

$M_{ox}, g_{i_{ox}}, g_{de_{ox}}, g_{s_{ox}}, \dot{m}_{ox}, \dot{m}_i, \dot{m}_r, \dot{m}_s$

Other 5 (auxiliary) equations in this block, including the gas state equation and its internal energy and mixture mass relationships, allow the substitution of the above state variables with the three controlled state variables of this element: pressure, temperature and O_2 concentration $(p_b, T_b, g_{s_{ox}})$.

Block 3 - Exhaust gas cooler, water condenser and separator (WC and WS in Fig. 1)

3.1: mass balance

$$\frac{dM_{g_{sc}}(p_c)}{d\tau} = \dot{m}_e - \dot{m}_{el} - \dot{m}_{H_2O}$$

$M_{g_{sc}}, \dot{m}_e, \dot{m}_{el}, \dot{m}_{H_2O}$

Other 12 (auxiliary) equations in this block, including the gas state equation and its internal energy and mixture mass functions, define the relationship between the above state variable $(M_{g_{sc}})$ with the WS pressure (p_c), used as the controlled state variable and define the cool dry gas thermodynamic properties.

Blocks 4 to 6 - Closed loop by-pass node

These correspond to 3 auxiliary equations defining the pressure drop along the pipe from the WS to the OMM (by-pass), and the gas and O_2 mass conservation in the node which allow the calculation of gas mass flow rate, gas constant (R) and O_2 concentration in the streams going to the LLC and the OMM.

Equations | Time dependant variables

Block 7 - Compressor and post compression cooler (LLC and WC in Fig. 1)

7.1: shaft balance

$$\frac{dn_c}{d\tau} = \frac{60}{2\pi J_c}\left(C_{m_c} - C_{r_c}\right) \qquad n_c, C_{m_c}, C_{r_c}$$

Other 13 (auxiliary) equations in this block allow the calculation of the compression work, efficiency and consequent compressor's shaft torque (C_{r_c}) and speed (n_c), as function of the properties and flow rate of the cool dry gas to be compressed and of the pressure in the CO_2 liquefaction system and vessel. Post compression and post water cooling and temperatures realationships belong to this block also.

Block 8 - Compressor's electric motor

This block of 3 auxiliary equations define the realationship between the controlled input voltage of the motor and the torque generated (C_{m_c}).

Block 9 - Overall refrigeration system (the semi-open system made of the liquid O_2 and the CO_2 liquefaction and storage systems)

9.1: overall enthalpy balance

$$\frac{d}{d\tau}\left(U_{ox_s} + U_{cd_s}\right) = \dot{m}_{de}\, h_1 - \dot{m}_i\, h_4 + \dot{m}_{ox}\, h_3 + Q_{ox_s} + Q_{cd_s} \qquad U_{ox_s}, U_{cd_s}, h_1, h_4, h_s, \dot{m}_{de}, \dot{m}_i, \dot{m}_{ox}, Q_{ox_s}, Q_{cd_s},$$

Other 11 (auxiliary) equations in this block, including the internal energy relationships of the two gas mixtures, the heat leakage and the enthalpies functions, relate the above variables with the controlled state variable (T_{sc}) and the following: temperature in the O_2 vessel (T_{so}) and O_2 concentration at the inlet and outlet of the CO_2 vessel ($g_{de_{ox}}$, $g_{i_{ox}}$).

Block 10 - Liquid O_2 vessel (SO in Fig. 1)

10.1: mass balance

$$\frac{dM_{ox_g}}{d\tau} = \dot{m}_{ox} - \dot{m}_{ox_{evap}} \qquad M_{ox_g}, \dot{m}_{ox}, \dot{m}_{ox_{evap}}$$

The other 2 (auxiliary) equations in this block are the O_2 state equation and its temperature-pressure relationship, which relate the above variables with the temperature (T_{so}) and the pressure (p_{so}) in the O_2 vessel.

Equations

Time dependant variables

Block 11 - Liquid CO_2 vessel

11.1: mass balance

$$\frac{dM_{gcd}}{d\tau} = \dot{m}_{de} - \dot{m}_i - \dot{m}_{l_{cd}}$$

M_{gcd}, $\dot{m}_{de}$, $\dot{m}_i$, $\dot{m}_{l_{cd}}$

Other 5 (auxiliary) equations in this block are the gas mixture mass and state equation, the gas mixture constant, the CO_2 partial pressure and the total pressure relationships with the O_2 concentration ($g_{i_{ox}}$) at the oulet (venting valve VI) of the CO_2 vessel.

Blocks 12 to 15 - Heat exchangers and control valves equations

These 52 auxiliary equations include the following sets:

- the enthalpy balance, the relationships between enthalpy, temperature, mass and molar concentrations in the main sections of the O_2 superheater (OSH in Fig.1),
- the equations for the calculation of the heat exchange coefficient in the various sections of the OSH,
- the enthalpy balance, the relationships between enthalpy, temperature, mass and molar concentrations in the main sections of the O_2 evaporator (inside the CO_2 vessel in Fig.1),
- the equations for the calculation of the heat exchange coefficient and the vaporized mass flow rate in the O_2 evaporator,
- the O_2 control valve (OCV) equations,
- the liquid O_2 control valve (V_{LOX}) equations,
- the uncondensated gas control valve (VI) equations.

Blocks R1 to R3 - Regulators

These blocks include:

- 1 differential equation of the PI regulator of the engine speed (n) with 3 auxiliary equations,
- 2 differential equations of the PID regulator of the O_2 concentration in the OMM ($g_{s_{ox}}$) with 4 auxiliary equations,
- 2 auxiliary equations of the P regulator of the CO_2 vessel pressure (p_{sc})
- 2 auxiliary equations of the P regulator of the closed loop pressure (p_c)

NOMENCLATURE

Symbols	Units	Definitions
C_m	Nm	Engine torque
C_{m_c}	Nm	Compressor motor torque
C_r	Nm	Load torque
C_{r_c}	Nm	Compressor load torque
$g_{de_{ox}}$	kg/kg	Oxygen mass concentration in the dehydrated, recirculated gas (from the WS)
$g_{i_{ox}}$	kg/kg	Oxygen mass concentration in the uncondensated gas
$g_{s_{ox}}$	kg/kg	Oxygen mass concentration in the gas at the engine inlet (OMM outlet)
g_r	-	Engine regulation ratio
h_1	kJ/kg	Specific enthalpy of the compressed gas at the compressor outlet (OSH inlet)
h_3	kJ/kg	Specific enthalpy of the superheated oxygen (OSH outlet)
h_4	kJ/kg	Specific enthalpy of the uncondensated gas (CO_2 vessel outlet)
h_r	kJ/kg	Specific enthalpy of the recirculated gas (WS outlet)
h_s	kJ/kg	Specific enthalpy of the gas at the engine inlet manifold
J	kg m^2	Engine and load moment of inertia (reduced at the engine shaft)
J_c	kg m^2	Compressor and motor moment of inertia (reduced at the compressor shaft)
$\dot{m}_e$	kg/s	Gas mass flow rate from the engine oulet manifold (WC and WS inlet)
$\dot{m}_{e_1}$	kg/s	Recirculated, cool gas mass flow rate at the WS outlet
$\dot{m}_{H_2O}$	kg/s	Condensed water mass flow rate (drained from WS)
$\dot{m}_i$	kg/s	Uncondensated gas mass flow rate from the CO_2 vessel to the OMM
$\dot{m}_{l_{cd}}$	kg/s	Overall rate of CO_2 liquified (OSH and CO_2 vessel)
$\dot{m}_r$	kg/s	Recirculated, cool gas mass flow rate going to the OMM
$\dot{m}_s$	kg/s	Gas mass flow rate to the engine inlet manifold
$\dot{m}_{de}$	kg/s	Gas mass flow rate delivered by the compressor
$\dot{m}_{ox}$	kg/s	Oxygen mass flow rate from the oxygen tank to the OMM
$\dot{m}_{ox_{evap}}$	kg/s	Rate of oxygen vapour produced in the evaporator
M_b	kg	Total gas mass in the oxygen mixing manifold
$M_{g_{cd}}$	kg	Total gas mass in the CO_2 vessel
$M_{g_{sc}}$	kg	Total gas mass in the exhaust gas cooler, water condenser and separator
M_{ox}	kg	Total oxygen mass in the oxygen mixing manifold
M_{ox_g}	kg	Oxygen saturated vapour mass in the LOX vessel
n	rpm	Engine speed
n_c	rpm	Compressor speed (LLC)
p_b	bar	Total gas pressure in the oxygen mixing manifold
p_c	bar	Total gas pressure in the exhaust gas cooler, water cond. & separ. (WC & WS)
p_{s_o}	bar	Pressure in the liquid O_2 vessel

p_{sc}	bar	Pressure in the CO_2 vessel
Q_{cd_s}	kW	Heat leakage into the CO_2 vessel
Q_{ox_s}	kW	Heat leakage into the oxygen vessel
T_b	K	Temperature in the oxygen mixing manifold
T_{sc}	K	Temperature of the liquid CO_2 in the CO_2 vessel
T_{so}	K	Temperature of the liquid O_2 in the O_2 vessel
U_b	kJ	Total internal energy of the gas in the OMM
U_{cd_s}	kJ	Total internal energy in the CO_2 vessel
U_{ox_s}	kJ	Total internal energy in the Oxygen vessel

USEFUL PEAK POWER	12	kW
USEFUL AVERAGE POWER	7.5	kW
MINIMUM CONTINUOUS POWER	2.5	kW
USEFUL ENERGY AUTONOMY	600	kWh
MAX OPERATIVE WATER DEPTH	6000	m

Tab. 1 - Energy and power requirements for an autonomous ROV

Compressor mass flow rate coefficient	f	1.3	-
Cooling water temperature	T_e	15	°C
Oxygen mass concentration at the engine inlet manifold (regulator set point)	g_{sox}	23	%
Closed circuit pressure (regulator set point)	p_c	1.05	bar
Liquid oxygen pressure control set point	p_{so}	1.5	bar
temperature	T_{so}	-178	°C

Tab. 2 - General fixed input data of the simulations.

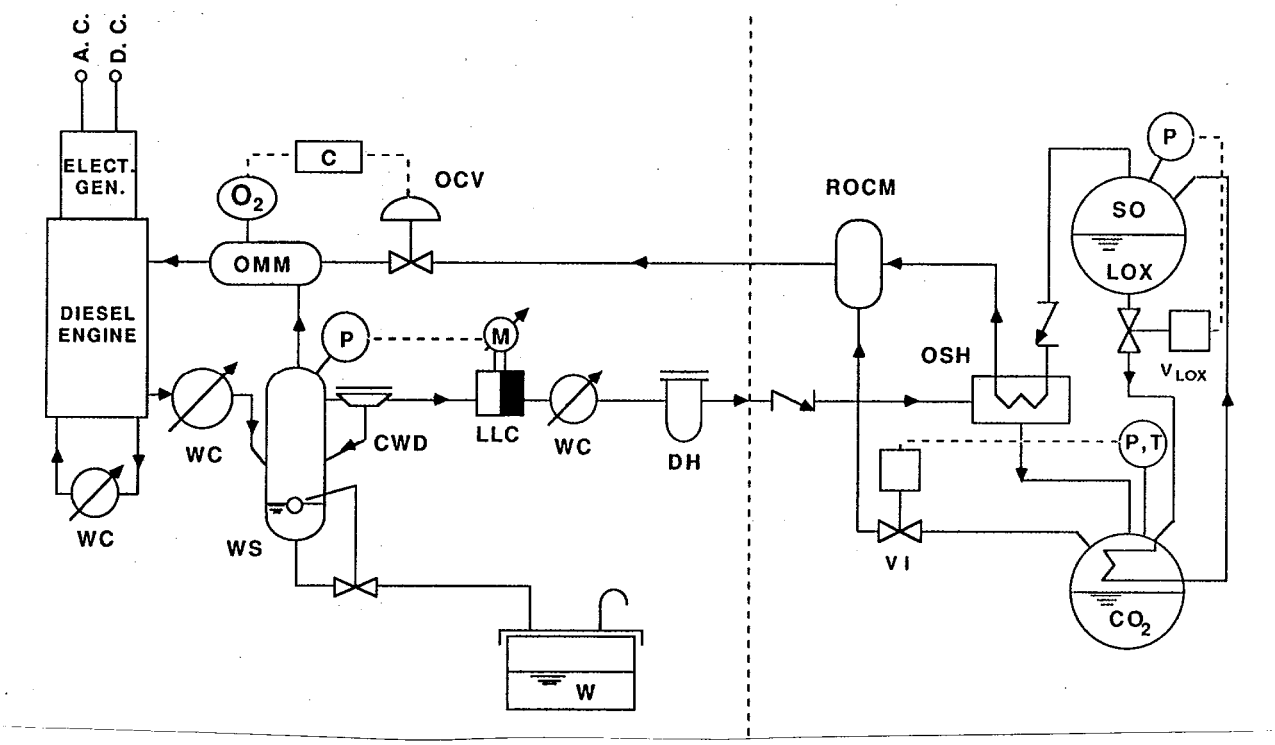

M	Compressor's, variable speed electric motor	O_2	Oxygen concentration transducer
LLC	Liquefaction loop compressor	C	Oxygen feeding controller
WC	Water cooled heat exchanger	OCV	Oxygen Control Valve
WS	Water separator	SO	Liquid oxygen storage vessel
CWD	Condensed water drainage	V_{LOX}	Liquid oxygen control valve
DH	De-hydrating filter	OSH	Oxygen superheater and CO_2 1st stage cooler and condenser
W	Combustion water storage tank	VI	Incondensated gas venting control valve
OMM	Oxygen Mixing Manifold	P,T	Pressure & Temperature transducers
ROCM	Residual oxygen collecting manifold		

Fig. 1 - Simplified diagram of the "Cryo-thermal" closed cycle Diesel system (pressure reducers in the oxygen rich lines are not shown).

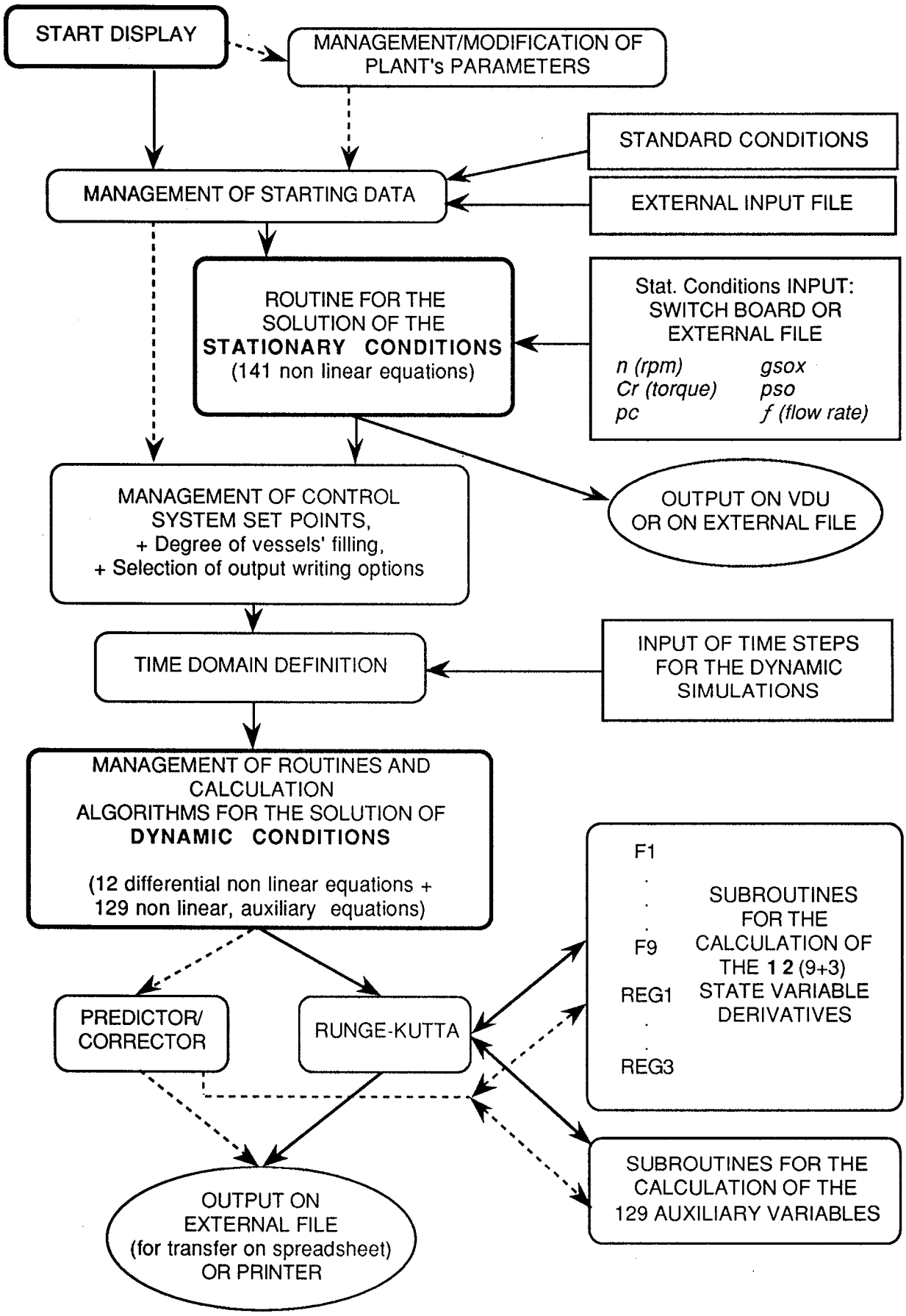

Fig. 2 - General block diagram of the "Cryo-thermal" simulation program.

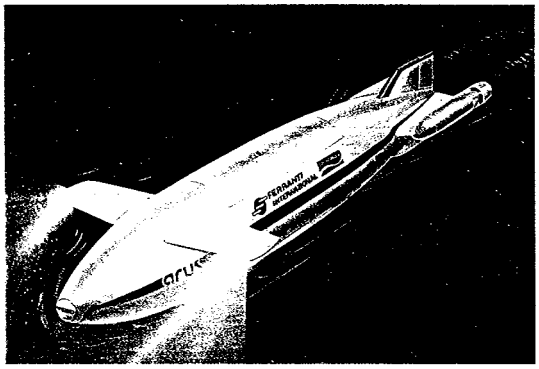

ARUS
(Autonomous Robot for Underwater Survey)

The ARUS will be a tetherless robot with onboard energy systems capable of carrying out also long range missions (250 hours).

Its operations will be autonomous and man-machine interface design will allow various interaction levels, from high level mission instructions to low level commands and readings.

dimensions	9 m and 1.2. m dia
displacement	100 kN
depth	6000 m
range	2000 km
duration	240 hours
speed (cruising)	2.5 m/s
propulsion	twin thrusters at tail
communication	acoustic during operation, 1.2 kb/s; UHF radio at surface, 1.2 kb/s
navigation	integrated inertial/acoustic velocity and EM logs; GPS updates when surfaced; acoustic LBL/USBL for survey
payload	side scan sonar swath bathymetry sub bottom profiler conductivity, temperature, depth echo sounder stereo camera gravimeter, magnetometer (opt.)

Fig. 3- Design case: AUV for long range surveys; the figure shows the characteristics of the ARUS vehicle, object of the EUREKA project EU 191, a cooperation between Tecnomare, ENEA and Ferranti International.

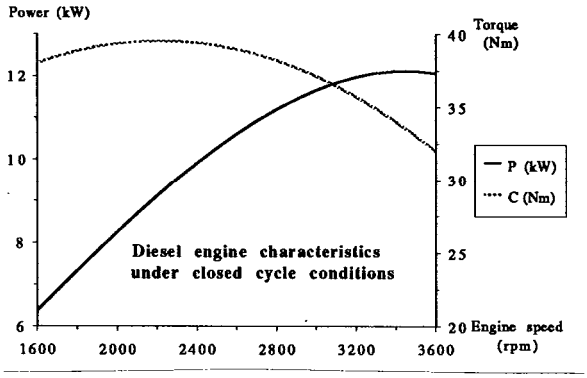

Fig. 4 - Engine torque-speed diagram, under closed cycle working conditions (CO_2/O_2 mixture)

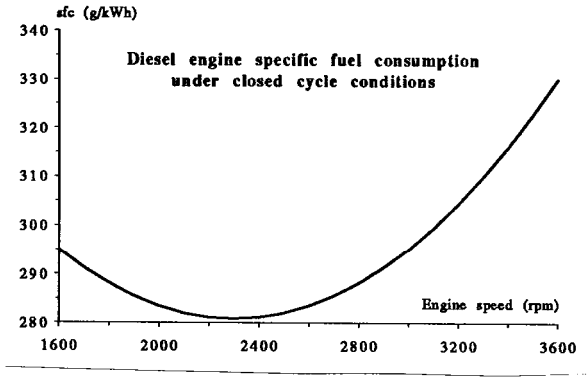

Fig. 5 - Engine specific fuel consumption under closed cycle working conditions (CO_2/O_2 mixture)

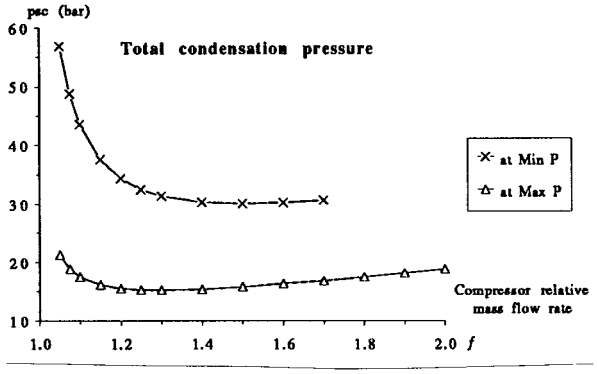

Fig. 6 - Total pressure in the CO_2 vessel as function of the mass flow coefficient f for min and max engine power.

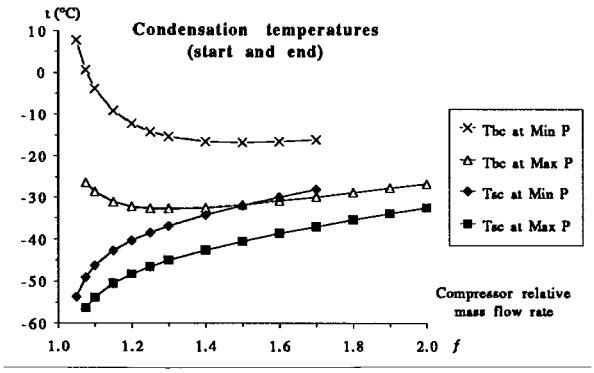

Fig. 7 - CO_2 condensation temperature in the 1st and 2nd cooling stages as function of the mass flow coefficient f for min and max engine power.

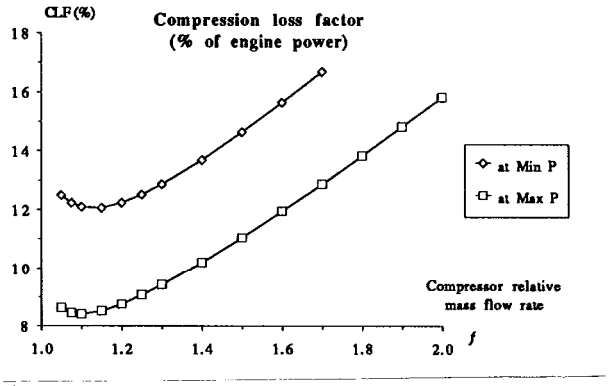

Fig. 8 - Compression loss factor (CLF) vs mass flow coefficient f for min and max engine power.

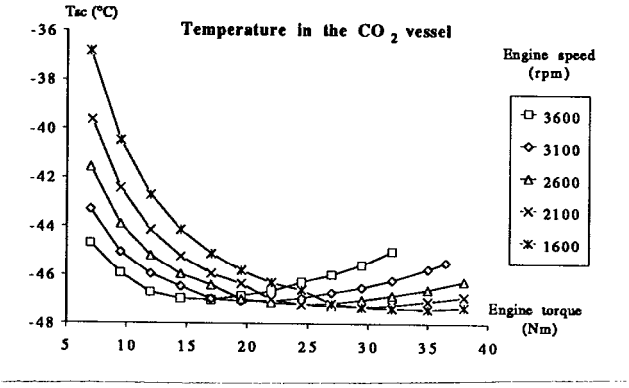

Fig. 11 - Temperature (T_{sc}) in the CO_2 vessel at the various engine load conditions.

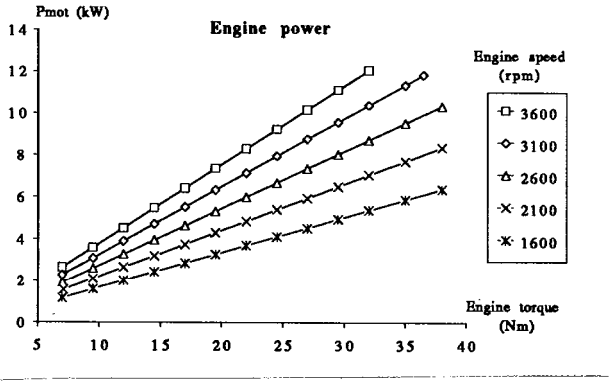

Fig. 9 - Stationary simulation cases: Engine power vs torque and speed set point.

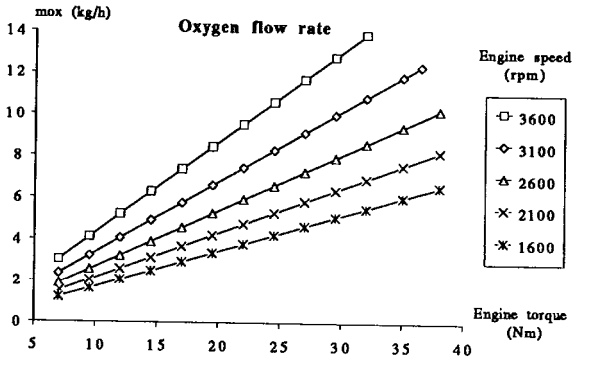

Fig. 12 - Oxygen flow rate (m_{ox}) at the various engine load conditions.

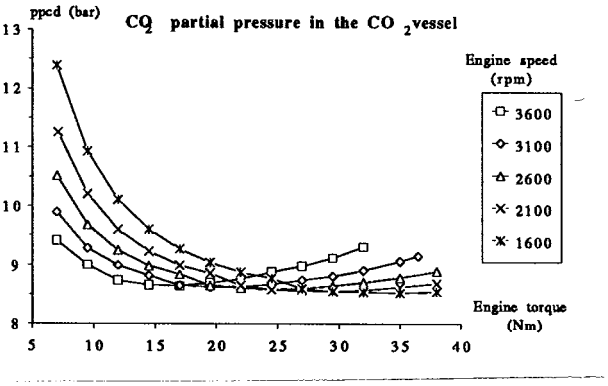

Fig. 10 - Partial CO_2 pressure (p_{pcd}) in the CO_2 vessel at the various engine load conditions.

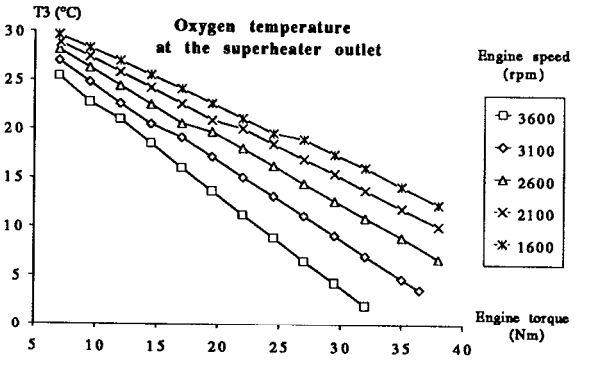

Fig. 13 - Superheated oxygen temperature (T_3) at the various engine load conditions.

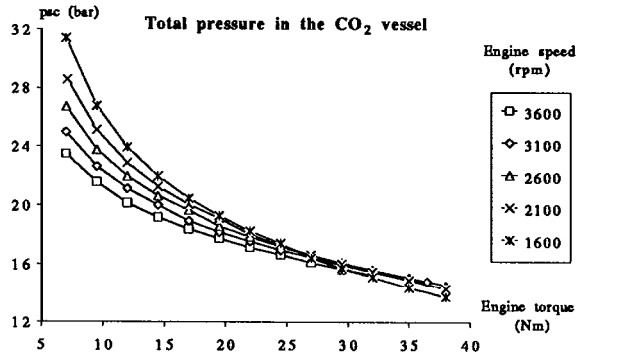

Fig. 14 - Total pressure of the gas mixture in the CO_2 vessel (p_{sc}) at the various engine load conditions.

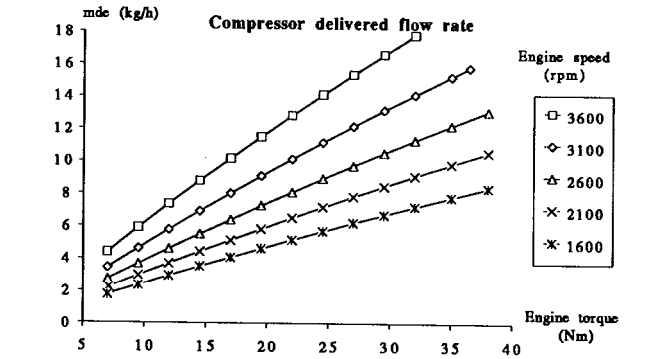

Fig. 17 - Gas flow rate delivered by the compressor (m_{de}) at the various engine load conditions.

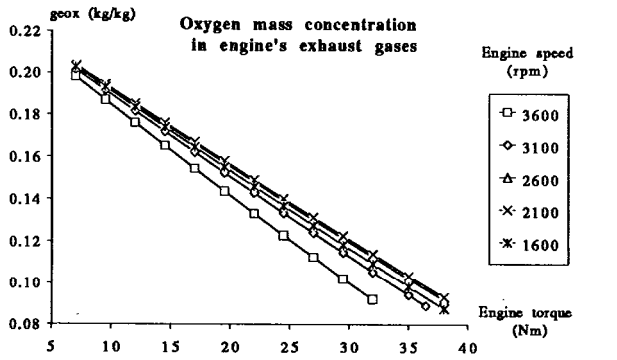

Fig. 15 - Oxygen mass concentration in engine's exhaust gases (g_{eox}) at the various engine load conditions.

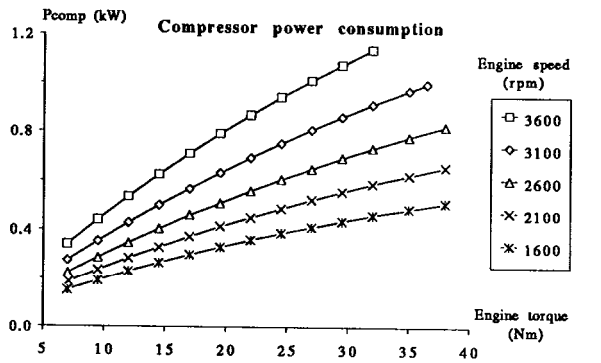

Fig. 18 - Compressor power consumption (P_{comp}) at the various engine load conditions.

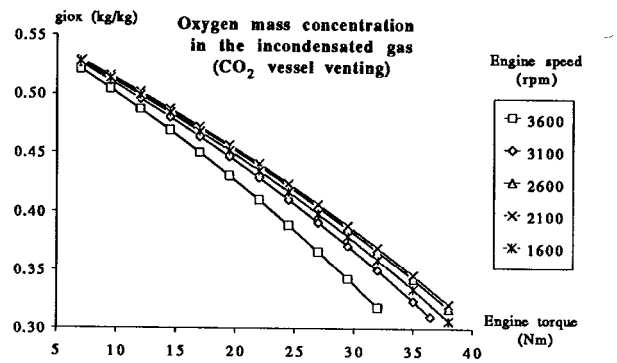

Fig. 16 - Oxygen mass concentration in the incondensated gases (g_{iox}) at the various engine load conditions.

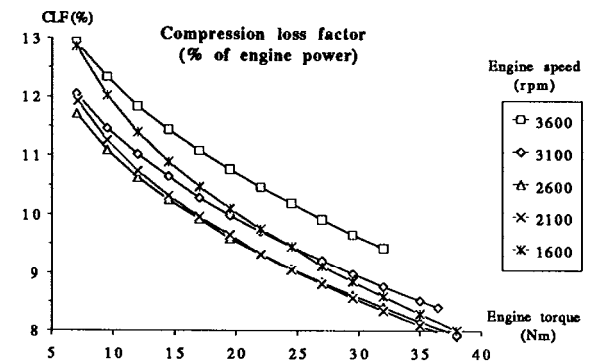

Fig. 19 - Compression loss factor (CLF) at the various engine load conditions.